

Symplectic tomographic probability distribution of crystallized Schrödinger cat states

Julio A. López-Saldívar^{1,2,3}, Margarita A. Man'ko⁴, and Vladimir I. Man'ko^{2,3,4}

¹*Instituto de Ciencias Nucleares, Universidad Nacional Autónoma de México, Apdo. Postal 70-543, Ciudad de México 04510, México*

²*Moscow Institute of Physics and Technology, Institutskii per. 9, Dolgoprudnyi, Moscow Region 141700, Russia*

³*Russian Quantum Center, Skolkovo, Moscow 143025, Russia*

⁴*Lebedev Physical Institute, Leninskii Prospect 53, Moscow 119991, Russia*

julio.lopez.8303@gmail.com

Abstract

Within the framework of the probability representation of quantum mechanics, we study a superposition of generic Gaussian states associated to symmetries of a regular polygon of n sides; in other words, the cyclic groups (containing the rotational symmetries) and dihedral groups (containing the rotational and inversion symmetries). We obtain the Wigner functions and tomographic probability distributions (symplectic and optical tomograms) determining the density matrices of the states explicitly as the sums of Gaussian terms. The obtained Wigner functions demonstrate nonclassical behavior, i.e., contain negative values, while the tomograms show a series of maxima and minima different for each state, where the number of the critical points reflects the order of the group defining the states. We discuss general properties of such a generalization of normal probability distributions.

1 Introduction

The states of quantum systems can be described by different approaches: as wave functions [1], as density matrices [2, 3], or using standard probability distributions called the tomographic representation of quantum states [4–6]. In particular, even and odd superpositions of Gaussian wave functions of standard coherent states (i.e., coherent states considered by Glauber [7] and Sudarshan [8]) have been very important for the development of quantum theory as they present non-classical behavior in spite of being the superposition of quasi-classical states. These states called even and odd Schrödinger cat states were studied in [9–11]. They have specific symmetry properties associated to the group of two elements – the identity and mirror reflection operations in the phase space. The even and odd coherent states were studied in the probability representation in [12, 13]. The states with other symmetries, such as crystallographic symmetries, were applied to Schrödinger cat states in [14–16]. In [17], different ways to detect the bipartite entanglement, using the tomographic probability representation, were presented. Additionally, it has been established that the generalization of the symmetric superposition of coherent states can be used as a qudit system as they are orthogonal between each other [18].

Several procedures have been proposed to obtain odd and even coherent states. For example, there was a proposal to generate low-photon-number cat states, also known as kitten states, in [19]. Other proposals have been made, namely, (i) to reflect a coherent pulse in an optical cavity with one atom [20, 21]; (ii) to detect a photon-number state [22] employing the ancilla-assisted photon subtraction [23]; (iii) to subtract a particular number of photons from a squeezed vacuum state [24] or to subtract one photon of a squeezed

vacuum state [25]. Nonclassical features of the superposition of coherent states like squeezing have been studied in [26–28]. The possible experimental implementation of these superpositions was mentioned in [29], and this implementation for coherent states on a circle was discussed in [26, 27, 30]. The circle states are connected with the phase–time operators in the problem of harmonic oscillator [31–34]. States with circle symmetry were defined in [35], using spin coherent states; also in [36], the $su(1, 1)$ coherent states on a hyperboloid were explored. A proposed method to generate states with high symmetry was studied by taking into account the dynamic evolution of a matter–field interaction described by the Tavis–Cummings Hamiltonian [37, 38].

The particular states studied in this work are associated to the symmetries of the regular n -sided polygon, in other words, superposition states resulting from the cyclic and dihedral group of operations over an initial state. The cyclic group $C_n = \mathbb{Z}/(n\mathbb{Z})$ is an abelian group, which elements are the operations associated to the rotation symmetries for a regular polygon. In other words, the n -degree cyclic group can be defined as $C_n = \{I, R(2\pi/n), R(4\pi/n), \dots, R(2(n-1)\pi/n)\}$, where $R(\theta)$ is the rotation operation. The cyclic group C_n has n irreducible representations denoted by $\lambda = 1, \dots, n$. The character $\chi_r^{(\lambda)}$ associated to the r th element of the group for the irreducible representation λ is given by one of the roots of unity.

The dihedral group D_n is a non-abelian group, with elements being the rotations and inversions associated to all the symmetries of the n -side regular polygon; in other words, $D_n = \{I, R(2\pi/n), \dots, R(2(n-1)\pi/n), M_1, \dots, M_n\}$, where M_j is the mirror reflection on the j th polygon symmetry axis.

It has been found [18] that a set of n orthogonal states associated to the cyclic and dihedral groups can be defined, using an initial, non-invariant state and its rotations plus reflections in the phase space. These states are defined by the sum of the rotated and inverted states, where the weight of each element in the sum is the character of the cyclic group representation.

The aim of this work is to define the Wigner functions and tomographic probability representation of the superposition of Gaussian states associated to the cyclic and dihedral groups defined in [18].

This paper is organized as follows.

In section 2, we review the approach of the tomographic representation of quantum mechanics from the viewpoint of the quantizer–dequantizer formalism. In section 3, we describe the symplectic-tomography representation for the superposition of coherent states associated to the C_3 group as an example. In section 4, we present the explicit expressions for the Wigner function and the tomogram for general superposition of Gaussian states, which have the cyclic and dihedral symmetries in the phase space; also here some general properties are discussed. Finally, in section 4, we present a summary of our work and concluding remarks.

2 Quantizer–dequantizer formalism

In order to describe the density operator by a function, which is a probability distribution, we consider the general method of an invertible mapping of operators acting in a Hilbert space onto functions called symbols of the operators. For an operator \hat{A} , let the set of operators $\hat{U}(x)$, called dequantizers, where $x = x_1, x_2, \dots, x_n$, to provide the function $f_A(x)$, due to the relationship

$$f_A(x) = \text{Tr} \left(\hat{A} \hat{U}(x) \right). \quad (1)$$

Let the other set of operators $\hat{D}(x)$, called quantizers, to provide the inverse relationship

$$\hat{A} = \int f_A(x) \hat{D}(x) dx. \quad (2)$$

The existence of a pair of operators $\hat{U}(x)$ and $\hat{D}(x)$ means that these operators satisfy the following condition for any operator \hat{A} :

$$f_A(x') = \int f_A(x) \text{Tr} \left(\hat{U}(x') \hat{D}(x) \right) dx; \quad (3)$$

a possibility to fulfill this condition is

$$\text{Tr} \left(\hat{U}(x') \hat{D}(x) \right) = \delta(x - x'). \quad (4)$$

Although it is not unique. For example, in the case of symplectic tomographic probability representation [4] of harmonic-oscillator states, one can describe the system with three variables $x = (x_1, x_2, x_3)$, where $x_1 = X$, $x_2 = \mu$, and $x_3 = \nu$ are real numbers, and the quantizer and dequantizer operators are defined as

$$\hat{U}(X, \mu, \nu) = \delta(X\hat{1} - \mu\hat{q} - \nu\hat{p}), \quad (5)$$

$$\hat{D}(X, \mu, \nu) = \frac{1}{2\pi} \exp[i(X\hat{1} - \mu\hat{q} - \nu\hat{p})], \quad (6)$$

with \hat{q} and \hat{p} being the position and momentum operators.

In this notation, the symbol (function associated to the density operator) corresponding to the density operator is $w(X | \mu, \nu)$; it is called symplectic tomogram and it can be written as

$$w(X | \mu, \nu) = \text{Tr}(\hat{\rho} \delta(X\hat{1} - \mu\hat{q} - \nu\hat{p})). \quad (7)$$

The symplectic tomogram can be used to reconstruct the density operator in view of the quantizer operator described above, namely,

$$\hat{\rho} = \frac{1}{2\pi} \int w(X | \mu, \nu) \exp[i(X\hat{1} - \mu\hat{q} - \nu\hat{p})] dX d\mu d\nu. \quad (8)$$

For the density operator $\hat{\rho} = |\psi\rangle\langle\psi|$ of the pure state $|\psi\rangle$, the tomogram $w(X | \mu, \nu)$ is expressed in terms of the wave function $\psi(y)$ as follows [39]:

$$w_\psi(X | \mu, \nu) = \frac{1}{2\pi|\nu|} \left| \int \psi(y) \exp\left[i\left(\frac{\mu y^2}{2\nu} - \frac{Xy}{\nu}\right)\right] dy \right|^2. \quad (9)$$

Recalling the physical meaning of the tomogram, we state that, for a normalized wave function $\psi(y)$, i.e., $\int |\psi(y)|^2 dy = 1$, the tomogram is a nonnegative normalized probability distribution of the variable X depending on real parameters μ and ν ; i.e., one has

$$\int w(X | \mu, \nu) dX = 1. \quad (10)$$

The real parameters $\mu = s \cos \theta$ and $\nu = s^{-1} \sin \theta$, determine the reference-frame of transformed axes in the phase space $\hat{q}' = \mu\hat{q} + \nu\hat{p}$ and $\hat{p}' = -\nu\hat{q} + \mu\hat{p}$, such that $[\hat{q}', \hat{p}'] = [\hat{q}, \hat{p}] = i\hat{1}$; $\hbar = 1$, which implies that the matrix $\begin{pmatrix} \mu & \nu \\ -\nu & \mu \end{pmatrix}$ is symplectic.

A classical analog of the symplectic tomogram is determined by the probability distribution $f(q, p)$ of a particle in the phase space, in view of the Radon transform, namely,

$$w_{\text{cl}}(X | \mu, \nu) = \int f(q, p) \delta(X - \mu q - \nu p) dq dp, \quad (11)$$

$$f(q, p) = \frac{1}{4\pi^2} \int w_{\text{cl}}(X | \mu, \nu) \exp[i(X - \mu q - \nu p)] dX d\mu d\nu. \quad (12)$$

The classical particle tomogram $w_{\text{cl}}(X | \mu, \nu)$ determines the probability distribution $f(q, p)$ and, being an analog of the quantum particle tomogram determined by the Wigner function, it reads

$$w(X | \mu, \nu) = \int W(q, p) \delta(X - \mu q - \nu p) \frac{dq dp}{2\pi}, \quad (13)$$

$$W(q, p) = \frac{1}{2\pi} \int w(X | \mu, \nu) \exp[i(X - \mu q - \nu p)] dX d\mu d\nu. \quad (14)$$

Here, for the particle pure state W_ψ , the Wigner function is

$$W_\psi(q, p) = \frac{1}{2\pi} \int \psi(q + u/2) \psi^*(q - u/2) e^{-ipu} du, \quad (15)$$

and it satisfies the normalization condition $\int W_\psi(q, p) \frac{dq dp}{2\pi} = 1$, for the normalized pure state.

In order to exemplify the standard procedure, we present an explicit definition of tomographic probability representation for the superposition of coherent states associated to the triangle rotation symmetries in the phase space.

3 Crystallized cat states on an example of the C_3 symmetry group

In [11], the even and odd coherent states were introduced, using the symmetry group C_2 , which is a set of the abelian group transformations applied to the Glauber coherent states $|\alpha\rangle$ of the harmonic oscillator; they provide two states (even and odd)

$$|\alpha_+\rangle = N_+ (|\alpha\rangle + |-\alpha\rangle), \quad N_+ = \left[2 \left(1 + e^{-2|\alpha|^2}\right)\right]^{-1/2}, \quad (16)$$

$$|\alpha_-\rangle = N_- (|\alpha\rangle - |-\alpha\rangle), \quad N_- = \left[2 \left(1 - e^{-2|\alpha|^2}\right)\right]^{-1/2}, \quad (17)$$

satisfying the equation

$$\hat{a}^2 |\alpha_\pm\rangle = \alpha^2 |\alpha_\pm\rangle, \quad \hat{a} = \frac{\hat{q} + i\hat{p}}{\sqrt{2}}. \quad (18)$$

The states under consideration can be generalized using the abelian symmetry group C_3 with three rotation elements 1 , $e^{2\pi i/3}$, and $e^{4\pi i/3}$ acting on the coherent states. It is the simplest generalization of the C_2 symmetry group, used for the definition of even and odd coherent states [11] and being the rotation group C_3 . In view of this symmetry group, we define the superposition of coherent states $|\alpha\rangle$ of the form

$$|\psi\rangle = N_3 (|\alpha\rangle + |\alpha e^{2\pi i/3}\rangle + |\alpha e^{4\pi i/3}\rangle), \quad (19)$$

where the identity irreducible representation of this group is used to obtain the coefficients in the sum of coherent states. The state $|\psi\rangle$ is a sum of three Gaussian states, i.e., the states with normalized wave functions $\langle\psi_i|\psi_j\rangle = 1$, given in the position representation by the expressions

$$\langle x|\psi_j\rangle = \psi_j(x) = \exp(A_j x^2 + B_j x + C_j); \quad j = 1, 2, 3, \quad (20)$$

and the superposition state vector reads

$$|\psi\rangle = \sum_{j=1}^3 D_j |\psi_j\rangle. \quad (21)$$

The normalization condition $\langle\psi|\psi\rangle = 1$ means that, for normalized states $\psi_j(x)$ giving the relations

$$C_j + C_j^* = \frac{1}{2} \ln \left(\frac{A_j + A_j^*}{\pi} \right) - \frac{(B_j + B_j^*)^2}{4(A_j + A_j^*)}, \quad (22)$$

the normalization of state (21) provides the connection for coefficients following from the equality

$$\langle\psi|\psi\rangle = \sum_{j,k=1}^3 D_j D_k^* \langle\psi_j|\psi_k\rangle = 1. \quad (23)$$

For states (20), the coefficients are

$$A_j = \frac{1}{2}, \quad B_j = \sqrt{2}\alpha e^{(2\pi i/3)j}, \quad C_j = -\frac{|\alpha|^2}{2} - \frac{[\alpha e^{(2\pi i/3)j}]^2}{2} \quad D_j = N_3; \quad j = 1, 2, 3. \quad (24)$$

Our aim is to obtain the tomographic probability distribution $w_\psi(X|\mu, \nu)$ for the state with the wave function $\psi(x)$ corresponding to the state vector (19).

Adopting the generic relation from [39], we write the tomogram in terms of Gaussian integrals as follows:

$$w_\psi(X|\mu, \nu) = \frac{1}{2\pi|\nu|} \left| \int dy \sum_{j=1}^3 D_j \exp(-A_j y^2 + B_j y + C_j) \exp\left(\frac{i\mu}{2\nu} y^2 - \frac{iX}{\nu} y\right) \right|^2, \quad (25)$$

where A_j , B_j , C_j , and D_j are given by (24). Then the tomogram for the state (19) can be written as

$$\begin{aligned}
w_\psi(X | \mu, \nu) &= \frac{1}{2\pi|\nu|} \left| N_1 e^{C_1} \sqrt{\frac{\pi}{A_1 - i\mu/2\nu}} \exp \frac{(B_1 - iX/2\nu)^2}{4(A_1 - i\mu/2\nu)} \right. \\
&\quad + N_2 e^{C_2} \sqrt{\frac{\pi}{A_2 - i\mu/2\nu}} \exp \frac{(B_2 - iX/2\nu)^2}{4(A_2 - i\mu/2\nu)} \\
&\quad \left. + N_3 e^{C_3} \sqrt{\frac{\pi}{A_3 - i\mu/2\nu}} \exp \frac{(B_3 - iX/2\nu)^2}{4(A_3 - i\mu/2\nu)} \right|^2. \tag{26}
\end{aligned}$$

Here, the coefficients N_j, A_j, B_j, C_j ; $j = 1, 2, 3$ are given as functions of complex parameters α describing Schrödinger cat states. In the case of an arbitrary superposition of N Gaussian states $|\psi\rangle = \sum_{j=1}^N N_j |\psi_j\rangle$, with the normalized state vector $|\psi_j\rangle$, the general formula for tomogram is a sum of normalized Gaussian terms,

$$w_\psi(X | \mu, \nu) = \frac{1}{2\pi|\nu|} \left| \sum_{j=1}^N N_j e^{C_j} \sqrt{\frac{\pi}{A_j - i\mu/2\nu}} \exp \frac{(B_j - iX/2\nu)^2}{4(A_j - i\mu/2\nu)} \right|^2. \tag{27}$$

These tomograms describe also states, which are the states of crystallized Schrödinger cat states corresponding to an arbitrary symmetry group.

4 General superpositions of Gaussian states associated to the cyclic and dihedral groups

The superposition of coherent states studied above is a particular case of a symmetric superposition of states. One can define more general cyclic or dihedral states by considering an initial state $|\phi\rangle$, which we assume to be non-invariant under rotations in the phase space (to define cyclic states) or non-invariant under rotations and inversions in the phase space (to define dihedral states) [18].

Given this non-invariant state $|\phi\rangle$, which is required to be non-invariant under the rotations in the phase space for now, we can define n states associated to the cyclic group of n degree as follows [18]:

$$|\psi_r^{(\lambda)}(\phi)\rangle = N_\lambda \sum_{j=1}^n \chi_r^{(\lambda)} \hat{R}(\theta_r) |\phi\rangle, \tag{28}$$

with λ being one of the n irreducible representations of the cyclic group. Here, the rotation operator is denoted by $\hat{R}(\theta_r) = e^{-i\theta_r \hat{n}}$ and the character of the group is $\chi_r^{(\lambda)} = e^{2\pi i(\lambda-1)(r-1)/n}$, with the rotation angle $\theta_j = 2\pi(j-1)/n$ and the normalization constant

$$N_\lambda^{-2} = \sum_{r,s=1}^n \chi_r^{(\lambda)} \chi_s^{(\lambda)*} \langle \phi | \hat{R}^\dagger(\theta_s) \hat{R}(\theta_r) | \phi \rangle. \tag{29}$$

This state has an associated Wigner function, which can be obtained by the following integral:

$$W_\lambda(x, p) = \frac{1}{2\pi\hbar} \int d\xi e^{-(i/\hbar)p\xi} \psi_\lambda^* \left(x - \frac{1}{2}\xi \right) \psi_\lambda \left(x + \frac{1}{2}\xi \right).$$

In the case of the cyclic states, $W_\lambda(x, p)$ takes the form

$$W_\lambda(x, p) = \frac{N_\lambda^2}{2\pi\hbar} \sum_{r,s=1}^n \int_{-\infty}^{\infty} d\xi e^{-(i/\hbar)p\xi} \chi_r^{(\lambda)*} \chi_s^{(\lambda)} \phi_r^* \left(x - \frac{1}{2}\xi \right) \phi_s \left(x + \frac{1}{2}\xi \right), \tag{30}$$

with $\phi_j(x) = \langle x | \hat{R}(\theta_j) | \phi \rangle$.

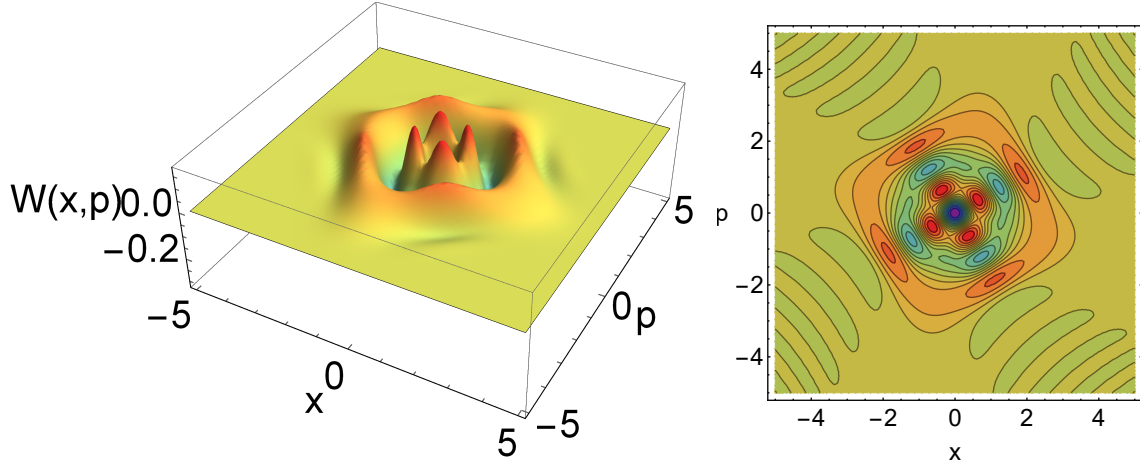


Figure 1: Wigner function for the cyclic state of fourth order with irreducible representation $\lambda = 1$ (left) and its contour plot (right). Here, the parameters $a = 1$ and $b = \sqrt{2}(1 + i)$ are taken.

For the cyclic Gaussian states [18] associated to the initial non-invariant state

$$\phi(x) = \left(\frac{a + a^*}{\pi} \frac{1 + 2a}{1 + 2a^*} \right)^{1/4} e^{-\frac{b^2 + |b|^2}{4(a + a^*)}} e^{-ax^2 + bx}, \quad (31)$$

one can demonstrate that, in the position representation, its rotation in the phase space $\langle x | \hat{R}(\theta_j) | \phi \rangle$ is given by the following expression:

$$\phi_j(x) = \langle x | \hat{R}(\theta_j) | \phi \rangle = \left(\frac{a_j + a_j^*}{\pi} \frac{1 + 2a_j}{1 + 2a_j^*} \right)^{1/4} e^{-\frac{b_j^2 + |b_j|^2}{4(a_j + a_j^*)}} e^{-a_j x^2 + b_j x}, \quad (32)$$

where the parameters

$$a_j = \frac{2ia \cos \theta_j - \sin \theta_j}{2(i \cos \theta_j - 2a \sin \theta_j)}, \quad b_j = \frac{b}{\cos \theta_j + 2ia \sin \theta_j}$$

are taken into account. The normalization constant, in this case, is

$$N_\lambda^{-2} = \sum_{r,s=1}^n c_r c_s^* \sqrt{\frac{\pi}{a_r + a_s^*}} e^{\frac{(br + b_s^*)^2}{4(a_r + a_s^*)}}, \quad c_j = \chi_j^{(\lambda)} \left(\frac{a_j + a_j^*}{\pi} \frac{1 + 2a_j}{1 + 2a_j^*} \right)^{1/4} e^{-\frac{b_j^2 + |b_j|^2}{4(a_j + a_j^*)}}. \quad (33)$$

The integral part of the Wigner function of Eq. (30) can be obtained using the integral, defined as

$W_{r,s}(x, p) = \int_{-\infty}^{\infty} d\xi e^{-(i/\hbar)p\xi} \chi_r^{(\lambda)*} \chi_s^{(\lambda)} \phi_r^*(x - \xi/2) \phi_s(x + \xi/2)$, which reads

$$W_{r,s}(x, p) = 2 \sqrt{\frac{\pi}{a_r + a_s^*}} c_r^* c_s e^{-\frac{4a_r^* a_s}{a_r^* + a_s} x^2 - \frac{p^2}{(a_r^* + a_s)\hbar^2} + \frac{2ipx(a_s - a_r^*)}{\hbar(a_r^* + a_s)} + \frac{2(a_r^* b_s + a_s b_r^*)}{a_r^* + a_s} x + \frac{ip(b_r^* - b_s)}{\hbar(a_r^* + a_s)} + \frac{(b_r^* - b_s)^2}{4(a_r^* + a_s)}}. \quad (34)$$

The results obtained provide the possibility to obtain the cyclic Wigner function as follows:

$$W_\lambda(x, p) = \frac{N_\lambda^2}{2\pi\hbar} \sum_{r,s=1}^n W_{r,s}(x, p). \quad (35)$$

In Fig. 1, the Wigner function for the cyclic state associated to the cyclic group C_4 and irreducible representation $\lambda = 4$ is shown. In this figure, one can confirm the rotation symmetry in the phase space for rotations multiple of $\pi/2$: it is also seen that the inversion symmetry is not present as that symmetry is not present in the cyclic group. Analogously, the pentagon rotation symmetry can be seen in the Wigner function presented in Fig. 2.

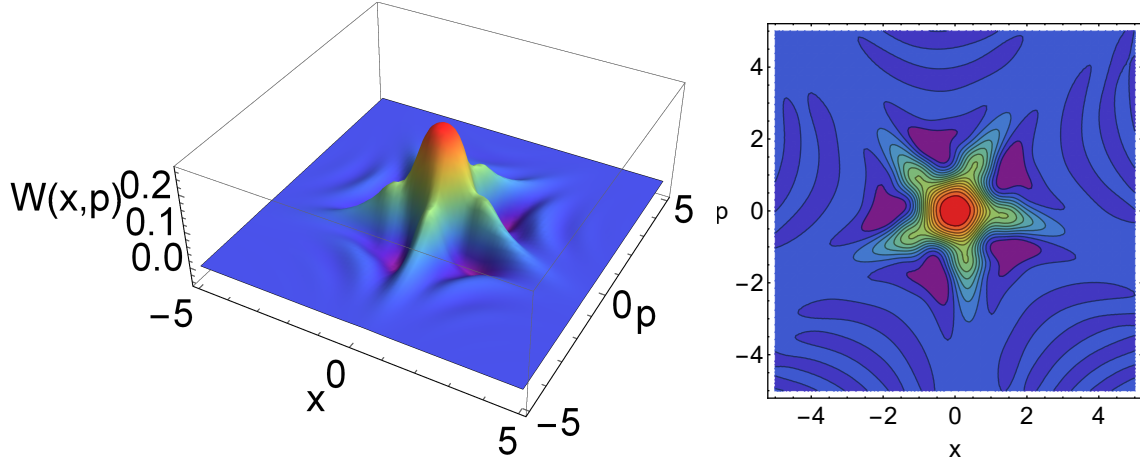


Figure 2: Wigner function for the cyclic state of fifth order with irreducible representation $\lambda = 1$ (left) and its contour plot (right). Here, the parameters $a = 2$ and $b = \sqrt{2}(1 - i)$ are taken.

In addition to the cyclic states, we present the Wigner function for the dihedral states of degree n , which have the same symmetries as the dihedral group D_n in the phase space. In other words, they are invariant under the rotations of the cyclic group and also under certain inversions, just like a regular polygon of n sides. The dihedral states are defined as [18]

$$|\gamma_r^{(\lambda)}(\phi)\rangle = N_\lambda \sum_{r=1}^n (\chi_r^{(\lambda)} \hat{U}_r |\phi\rangle + \chi_r^{(\lambda)*} \hat{U}_r^* |\phi^*\rangle), \quad (36)$$

with the dihedral group operator $\hat{U}_r = \hat{C} \hat{R}(\theta_r)$ being composed of a rotation \hat{R} and the complex conjugation \hat{C} . The characters $\chi_r^{(\lambda)} = e^{\frac{2\pi i(\lambda-1)(r-1)}{n}}$ are the ones for the cyclic subgroup. Then the Wigner function associated to these states is defined as

$$W(x, p) = \frac{N_\lambda^2}{2\pi\hbar} \sum_{r,s=1}^n \int_{-\infty}^{\infty} d\xi e^{-ip\xi/\hbar} \left\langle x - \frac{1}{2}\xi \left| (\chi_r^{(\lambda)} \hat{U}_r |\phi\rangle + \chi_r^{(\lambda)*} \hat{U}_r^\dagger |\phi^*\rangle) (\chi_s^{(\lambda)*} \langle\phi| \hat{U}_s^\dagger + \chi_s^{(\lambda)} \langle\phi^*| \hat{U}_s) \right| x + \frac{1}{2}\xi \right\rangle. \quad (37)$$

In the case of Gaussian dihedral states defined by the initial non-invariant state in Eq. (31), the Wigner function can be calculated with the help of the integral of Eq. (34) along with the following integrals:

$$W'_{r,s}(x, p) = \int_{-\infty}^{\infty} d\xi e^{-ip\xi/\hbar} \phi_r^* \left(x - \frac{1}{2}\xi \right) \phi_s^* \left(x + \frac{1}{2}\xi \right), \quad (38)$$

$$W''_{r,s}(x, p) = \int_{-\infty}^{\infty} d\xi e^{-ip\xi/\hbar} \phi_r \left(x - \frac{1}{2}\xi \right) \phi_s^* \left(x + \frac{1}{2}\xi \right), \quad (39)$$

$$W'''_{r,s}(x, p) = \int_{-\infty}^{\infty} d\xi e^{-ip\xi/\hbar} \phi_r \left(x - \frac{1}{2}\xi \right) \phi_s \left(x + \frac{1}{2}\xi \right). \quad (40)$$

In order to calculate these integrals, we point out that they are analogous to Eq. (34) with some replacements. For example, $W'_{r,s}(x, p)$ is equal to the expression of $W_{r,s}(x, p)$ with the replacements: $a_s \rightarrow a_s^*$, $a_s^* \rightarrow a_s$, $b_s \rightarrow b_s^*$, and $b_s^* \rightarrow b_s$. In view of this type of identification, the Wigner function for the dihedral states can be written as

$$W(x, p) = \frac{N_\lambda^2}{2\pi\hbar} \sum_{r,s=1}^n (W_{r,s}(x, p) + W'_{r,s}(x, p) + W''_{r,s}(x, p) + W'''_{r,s}(x, p)). \quad (41)$$

In Fig. 3, the Wigner function for the dihedral state of fourth order (D_4) is shown. One can see that the obtained quasiprobability distribution has both the rotational and inversion symmetries opposed to the ones seen in Fig. 1 for the cyclic group of the same degree. In a similar way, the Wigner function in Fig. 4 has the pentagon symmetries of D_5 , both rotational and inversion instead of only the rotational ones for the cyclic case seen in Fig. 2.

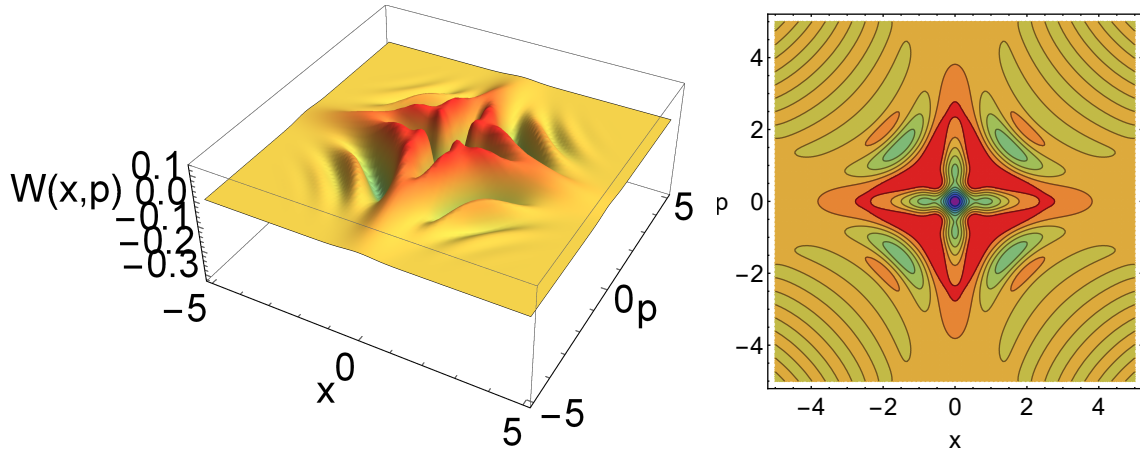


Figure 3: Wigner function for the dihedral state of fourth order with irreducible representation $\lambda = 2$ (left) and its contour plot (right). The parameters $a = 1$ and $b = \sqrt{2}(1 + i)$ were taken.

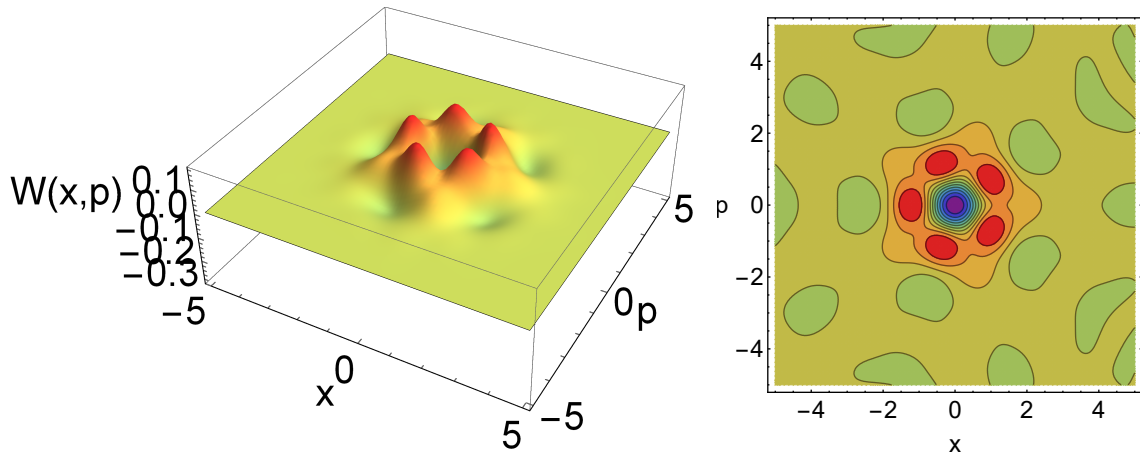


Figure 4: Wigner function for the dihedral state of fifth order with irreducible representation $\lambda = 2$ (left) and its contour plot (right). Here, the parameters $a = 2$ and $b = \sqrt{2}(1 - i)$ were taken.

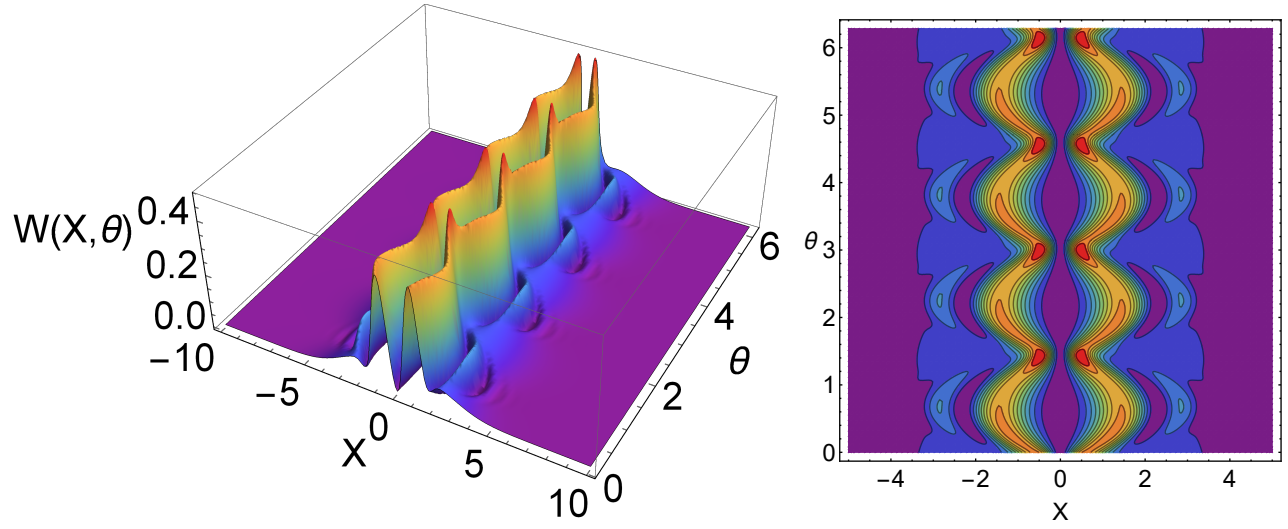


Figure 5: Tomographic representation for the cyclic state of fourth order C_4 associated to the irreducible representation $\lambda = 2$ (left) and its contour plot (right). The parameters $a = 2$, $b = 2(1 + i)$, and $s = 1$ were considered.

5 Tomographic representation for cyclic and dihedral states

As previously stated, the tomogram of a quantum system is the probability distribution for the position X in a rotated and rescaled coordinate system. In general, this tomogram can be calculated from the Wigner function and, in the case of the cyclic states, the tomographic representation of the states takes the form

$$w_\lambda(X, \theta) = \int_{-\infty}^{\infty} W_\lambda(X(x, p), P(x, p)) dP = \frac{N_\lambda^2}{2\pi\hbar} \sum_{r,s=1}^n \int_{-\infty}^{\infty} W_{r,s}(X(x, p), P(x, p)) dP, \quad (42)$$

where $X(x, p) = xs \cos \theta + ps^{-1} \sin \theta$ and $P(x, p) = ps^{-1} \cos \theta - xs \sin \theta$. This integral provides the following result:

$$w_\lambda(X, \theta) = \frac{N_\lambda^2}{2\pi\hbar} \sum_{r,r'=1}^n w_{r,r'}(X, \theta), \quad (43)$$

with

$$w_{r,r'}(X, \theta) = \frac{2\pi c_r^* c_{r'} |s|}{\sqrt{(s^2 \cos \theta + 2ia_{r'} \sin \theta)(s^2 \cos \theta - 2i \sin \theta a_r^*)}} e^{-\frac{s^2 X^2 (a_r^* + a_{r'})}{(s^2 \cos \theta + 2ia_{r'} \sin \theta)(s^2 \cos \theta - 2i \sin \theta a_r^*)}} \times e^{X \left(\frac{sb_r^*}{s^2 \cos \theta - 2i \sin \theta a_r^*} + \frac{sb_{r'}}{s^2 \cos \theta + 2ia_{r'} \sin \theta} \right) + \frac{1}{2} \sin \theta \left(\frac{b_r^{*2}}{2 \sin \theta a_r^* + is^2 \cos \theta} + \frac{b_{r'}^2}{2a_{r'} \sin \theta - is^2 \cos \theta} \right)}. \quad (44)$$

In Figs. 5 and 6, the tomographic representation for the cyclic states of fourth order ($\lambda = 2$) and fifth order ($\lambda = 3$) are plotted in terms of the parameters X and θ . In these figures, we can see that the probability of having a specific value of X is split into fringes, and the number of fringes depends on the order of the cyclic group.

In a similar way as the Wigner function, the tomogram associated to the dihedral states can be obtained by the following formula:

$$w_\lambda(X, \theta) = \frac{N_\lambda^2}{2\pi\hbar} \sum_{r,r'=1}^n (w_{r,r'}(X, \theta) + w'_{r,r'}(X, \theta) + w''_{r,r'}(X, \theta) + w'''_{r,r'}(X, \theta)), \quad (45)$$

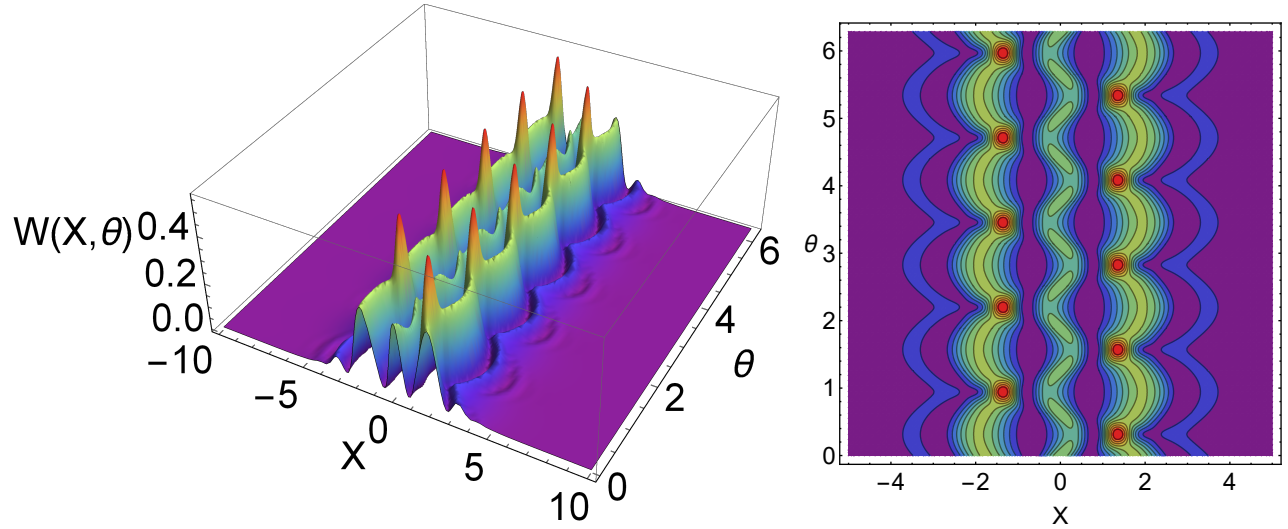


Figure 6: Tomographic representation for the cyclic state of fifth order C_4 associated to the irreducible representation $\lambda = 3$ (left) and its contour plot (right). Here, the parameters $a = 2$, $b = 2i$, and $s = 1$ were used.

with the following integrals:

$$w'_{r,r'}(X, \theta) = \int_{-\infty}^{\infty} W'_{r,r'}(X, P) dP, \quad w''_{r,r'}(X, \theta) = \int_{-\infty}^{\infty} W''_{r,r'}(X, P) dP, \quad w'''_{r,r'}(X, \theta) = \int_{-\infty}^{\infty} W'''_{r,r'}(X, P) dP. \quad (46)$$

Analogously to the Wigner function case mentioned above, the expressions for $w'_{r,r'}$, $w''_{r,r'}$, and $w'''_{r,r'}$ can be directly calculated from Eq. (44) by making the proper substitutions.

Some examples of the resulting tomograms for the dihedral groups of fourth and fifth order are shown in Figs. 7 and 8. One can see that, as in the cyclic case, for those states, the probability of having a certain value for the tomographic variable X can be divided into different fringes, where the probability of fringes depends on the degree of the dihedral group associated to the symmetric states.

6 Summary and concluding remarks

We point out the main results of our work. The symmetric superposition of cyclic and dihedral states were obtained in the probabilistic representation of quantum mechanics. In this representation, as an alternative of the standard description of quantum system states given by complex wave functions or density operators acting on the vectors of Hilbert spaces, the usual probability distributions, also known as tomograms, determine the states [4, 6]. We studied particular states of systems with continuous variables like oscillators and considered Gaussian state superpositions, since the probability distributions of such states are either normal probability distributions or sums of the Gaussian terms, which have not been discussed in the literature but are considered here as examples of Schrödinger cat states.

We reviewed the tomographic probability representation of quantum states and its properties. The particular representation for the superposition of coherent states for the cyclic group C_3 was explicitly addressed. Then the Wigner quasiprobability distribution associated to the cyclic and dihedral groups for a superposition of generic states was presented and used to obtain the tomographic probability representation of such states.

The obtained Wigner functions, for both cyclic and dihedral states, demonstrate nonclassical behavior as they contain negative values for different values of the position and momentum (or electromagnetic quadratures). This is due to the interference between two different rotations of the original Gaussian state, i.e., $\phi_j(x)$ and $\phi_{j'}(x)$ for $j \neq j'$ in the definition of Wigner function.

In the tomographic probability representation, the probability distribution for the parameter X is different from zero in a series of fringes as a function of the angle θ . The number of fringes depends on the degree of the cyclic or dihedral group, which defines a particular state.

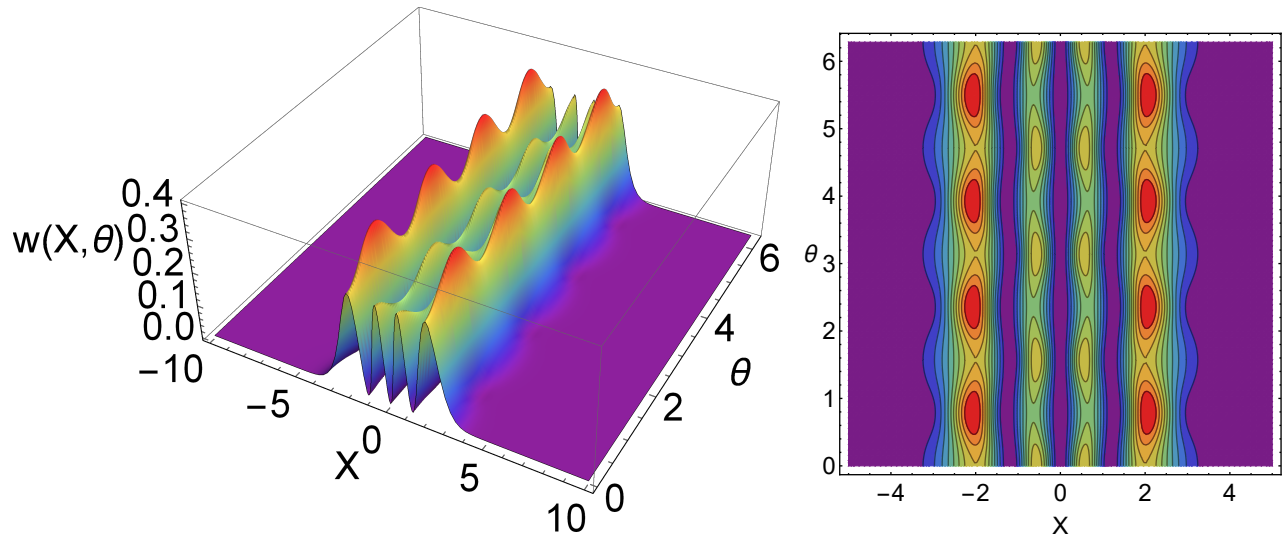


Figure 7: Tomogram for the dihedral state of fourth degree and irreducible representation $\lambda = 4$ as a function of X and θ (left) and its contour plot (right). Here, the parameters $a = 1$, $b = 1/2$, and $s = 1$ were taken.

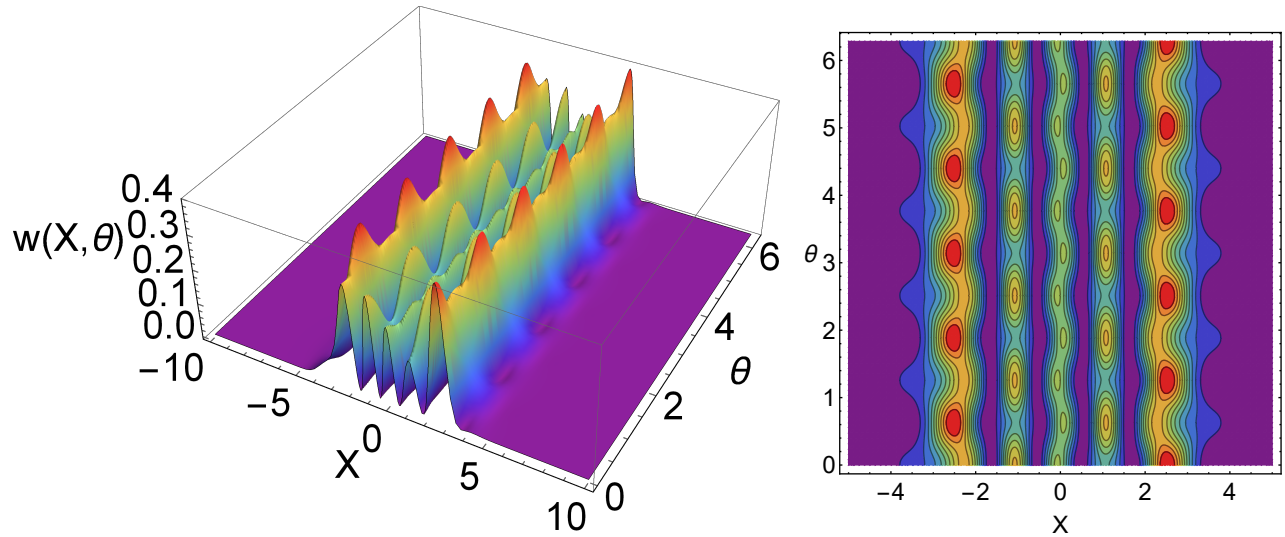


Figure 8: Tomogram for the dihedral state of fifth degree and irreducible representation $\lambda = 5$ as a function of X and θ (left) and its contour plot (right). Here, the parameters $a = 1$, $b = 1$, and $s = 1$ were used.

Acknowledgements

This work was partially supported by DGAPA-UNAM under Project IN101619. Results of Sections 2 and 3 were obtained by V.I.M and J.A.L.S in the Russian Quantum Center with the support from the Russian Science Foundation Grant No. 19-71-10091.

References

- [1] E. Schrödinger, Quantisierung als Eigenwertproblem (Zweite Mitteilung), *Ann. Phys.* **384** 361 and 489 (1926). doi:10.1002/andp.19263840404
- [2] L. Landau, Das Dämpfungsproblem in der Wellenmechanik, *Z. Phys.* **45** 430 (1927).
- [3] J. von Neumann, Wahrscheinlichkeitstheoretischer Aufbau der Quantenmechanik, *Gött. Nach.* 245 (1927). J. von Neumann, *Mathematical foundations of Quantum Mechanics* (Princeton University Press, USA), 1955.
- [4] S. Mancini, V. I. Man'ko, and P. Tombesi, Symplectic tomography as classical approach to quantum systems, *Phys. Lett. A* **213(1)** 1 (1996). doi:10.1016/0375-9601(96)00107-7
- [5] M. Asorey, A. Ibort, G. Marmo, and F. Ventriglia, Quantum tomography twenty years later, *Phys. Scr.* **90(7)** 074031 (2015). doi:10.1088/0031-8949/90/7/074031
- [6] O. V. Man'ko and V. I. Man'ko, Probability representation of quantum states, *Entropy* **23(5)** 549 (2021). doi:10.3390/e23050549
- [7] R. J. Glauber, Coherent and incoherent states of the radiation field, *Phys. Rev.* **131** 2766 (1963). doi:10.1103/PhysRev.131.2766
- [8] E. C. G. Sudarshan, Equivalence of semiclassical and quantum mechanical descriptions of statistical light beams, *Phys. Rev. Lett.* **10** 277 (1963). doi:10.1103/PhysRevLett.10.277
- [9] Barry C. Sanders, Entangled coherent states, *Phys. Rev. A* **45** 6811 (1992); Erratum, *Phys. Rev. A* **46** 2966 (1992). doi:10.1103/PhysRevA.45.6811
- [10] B. C. Sanders, Review of entangled coherent states, *J. Phys. A: Math. Theor.* **45(24)** 244002 (2012). doi:10.1088/1751-8113/45/24/244002
- [11] V. V. Dodonov, I. A. Malkin, and V. I. Man'ko, Even and odd coherent states and excitations of a singular oscillator, *Physica* **72(3)** 597 (1974). doi:10.1016/0031-8914(74)90215-8
- [12] S. V. Kuznetsov, A. V. Kyusev, O. V. Man'ko, and N. V. Chernega, Tomography and statistical properties of superposition states for two-mode systems, *Bulletin of the Russian Academy of Science, Physics*, Alerton Press Inc., Vol. 68, No 9, pp. 1239-1243 (2004) [in Russian]. <https://www.elibrary.ru/item.asp?id=17641248> [Translated into English by Pleiades Publishing and distributed by Springer (Springer Nature Switzerland AG)].
S. V. Kuznetsov, A. V. Kyusev, O. V. Man'ko, Tomography and statistical properties of superposition states for two-mode systems, *Proc. SPIE*, Vol. 5402, International Workshop on Quantum Optics 2003, St.-Peterburg (2004) p. 314-327. doi:10.1117/12.562263
- [13] P. Ádám, M. A. Man'ko, and V. I. Man'ko, Even and odd Schrödinger cat states in the probability representation of quantum mechanics, *J. Russ. Laser Res.* **43** 1 (2022).
- [14] V. V. Dodonov and V. I. Man'ko, *Proceedings of the Lebedev Physical Institute* **183** (Commack, NY: Nova Science) (1989).
- [15] O. Castaños, R. López-Peña, and V. I. Man'ko, Crystallized Schrödinger cat states, *J. Russ. Laser Res.* **16** 477 (1995). doi:10.1007/BF02581033
- [16] O. Castaños and J. A. López-Saldívar, Dynamics of Schrödinger cat states, *J. Phys.: Conf. Ser.* **380** 012017 (2012). doi:10.1088/1742-6596/380/1/012017

- [17] J. A. López-Saldívar, A. Figueroa, O. Castañón, R. López-Peña, M. A. Man'ko, and V. I. Manko, Evolution and entanglement of Gaussian states in the parametric amplifier, *J. Russ. Laser Res.* **37** 23 (2016). doi:10.1007/s10946-016-9543-2
- [18] J. A. López-Saldívar, General superposition states associated to the rotational and inversion symmetries in the phase space, *Phys. Scri.* **95** 065206 (2020). doi:10.1088/1402-4896/ab7
- [19] A. Ourjoumtsev, R. Tualle-Brouri, J. Laurat, and P. Grangier, Generating optical Schrödinger kittens for quantum information processing, *Science* **312** 83 (2006). doi:10.1126/science.1122858
- [20] B. Wang and L.-M. Duan, Engineering superpositions of coherent states in coherent optical pulses through cavity-assisted interaction, *Phys. Rev. A* **72** 022320 (2005). doi:10.1103/PhysRevA.72.022320
- [21] B. Hacker, S. Welte, S. Daiss, A. Shaukat, S. Ritter, L. Li, and G. Rempe, Deterministic creation of entangled atom-light Schrödinger-cat states, *Nature Photon.* **13** 110 (2019). doi:10.1038/s41566-018-0339-5
- [22] A. Ourjoumtsev, H. Jeong, R. Tualle-Brouri, and P. Grangier, Generation of optical Schrödinger cats from photon number states, *Nature* **448** 784 (2007). doi:10.1038/nature06054
- [23] H. Takahashi, K. Wakui, S. Suzuki, M. Takeoka, K. Hayasaka, A. Furusawa, and M. Sasaki, Generation of large-amplitude coherent-state superposition via ancilla-assisted photon subtraction, *Phys. Rev. Lett.* **101** 233605 (2008). doi:10.1103/PhysRevLett.101.233605
- [24] T. Gerrits, S. Glancy, T. S. Clement, B. Calkins, A. E. Lita, A. J. Miller, A. L. Migdall, S. W. Nam, R. P. Mirin, and E. Knill, Generation of optical coherent-state superpositions by number-resolved photon subtraction from the squeezed vacuum, *Phys. Rev. A* **82** 031802(R) (2010). doi:10.1103/PhysRevA.82.031802
- [25] J. S. Neergaard-Nielsen, B. Melholt Nielsen, C. Hettich, K. Mälmer, and E. S. Polzik, Generation of a superposition of odd photon number states for quantum information networks, *Phys. Rev. Lett.* **97** 083604 (2006). doi:10.1103/PhysRevLett.97.083604
- [26] J. Janszky, P. Domokos, and P. Ádám, Coherent states on a circle and quantum interference, *Phys. Rev. A* **48** 2213 (1993). doi:10.1103/PhysRevA.48.2213
- [27] P. Domokos, P. Ádám, and J. Janszky, One-dimensional coherent-state representation on a circle in phase space, *Phys. Rev. A* **50** 4293 (1994). doi:10.1103/PhysRevA.50.4293
- [28] V. Bužek, A. Vidiella-Barranco, and P. L. Knight, Superpositions of coherent states: Squeezing and dissipation, *Phys. Rev. A* **45** 6570 (1992). doi:10.1103/PhysRevA.45.6570
- [29] S. Szabo, P. Ádám, J. Janszky, and P. Domokos, Construction of quantum states of the radiation field by discrete coherent-state superpositions, *Phys. Rev. A* **53** 2698 (1996). doi:10.1103/PhysRevA.53.2698
- [30] J. A. González and M. A. del Olmo, Coherent states on the circle and quantization, *J. Phys. A* **31** 8841 (1998). doi:10.1088/0305-4470/31/44/012
- [31] L. Susskind and J. Glogower, Quantum-mechanical phase and time operator, *Physics Physique Fizika* **1** 49 (1964). doi:10.1103/PhysicsPhysiqueFizika.1.49
- [32] M. M. Nieto, Quantum phase and quantum phase operators: some physics and some history *Phys. Scr.* **T48** 5 (1993). doi:10.1088/0031-8949/1993/T48/001
- [33] D. T. Pegg and S. M. Barnett, Unitary phase operator in quantum mechanics, *Europhys. Lett.* **6** 483 (1988). doi:10.1209/0295-5075/6/6/002
- [34] D. T. Pegg and S. M. Barnett, Phase properties of the quantized single-mode electromagnetic field, *Phys. Rev. A* **39** 1665 (1989). doi:10.1103/PhysRevA.39.1665
- [35] M. Calixto, J. Guerrero, and J. C. Sánchez-Monreal, Sampling theorem and discrete Fourier transform on the Riemann sphere, *J. Fourier Anal. Appl.* **14** 538 (2008). doi:10.1007/s00041-008-9027-z
- [36] M. Calixto, J. Guerrero, and J. C. Sánchez-Monreal, Sampling theorem and discrete Fourier transform on the hyperboloid, *J. Fourier Anal. Appl.* **17** 240 (2011). doi:10.1007/s00041-010-9142-5

- [37] O. Castaños, S. Cordero, E. Nahmad-Achar, and R. López-Peña, Generation and dynamics of crystallised-type states of light within the Tavis–Cummings model. In: Duarte S., Gazeau J.-P., Faci S., Micklitz T., Scherer R., and Toppan F. (Eds.), *Physical and Mathematical Aspects of Symmetries* (Springer, Cham, 2017). doi:10.1007/978-3-319-69164-0_17
- [38] S. Cordero, E. Nahmad-Achar, O. Castaños, and R. López-Peña, Dynamic generation of light states with discrete symmetries, *Phys. Rev. A* **97**, 013808 (2018). doi:10.1103/PhysRevA.97.013808
- [39] V. I. Man’ko and R. Vilela Mendes, *Phys. Lett. A* **263** 53 (1999). doi:10.1016/S0375-9601(99)00688-X